Available online at www.sciencedirect.com
SCIENCE DIRECT®
Journal of Solid State Chemistry 174 (2003) 403–411
JOURNAL OF SOLID STATE CHEMISTRY
http://elsevier.com/locate/jssc

Pressure-induced metastable phase transition in orthoenstatite ($MgSiO_3$) at room temperature: a Raman spectroscopic study

Chung-Cherng Lin*

Institute of Earth Sciences, Academia Sinica, P.O. Box 1-55, Nankang, Taipei 115, Taiwan, ROC

Received 19 December 2002; received in revised form 21 April 2003; accepted 8 May 2003

Abstract

Phase behavior of a synthetic orthoenstatite in a diamond-anvil cell has been studied up to ~22 GPa by using Raman spectroscopy at room temperature. Under quasi-hydrostatic conditions, orthoenstatite undergoes a reversible phase transformation at an apparent transition pressure of ~10 GPa for compression and ~9.5 GPa for decompression. The 3*d* transition-metal cations, e.g., Fe^{2+} and Ni^{2+}, show only a minor effect on the transition pressure within 10 wt% of addition. All the Raman frequencies in both orthoenstatite and its high-pressure phase increase monotonically with increasing pressure. The amount of forward or backward transition is fixed at a given pressure and forms a hysteresis loop in the transition %-pressure plan. The type for the present metastable phase transition is inferred to be of first order and the high-pressure polymorph may be the intermediate between orthoenstatite and the high-pressure clinoenstatite (i.e., the high-P $C2/c$ phase). A mechanism based on Mnyukh's edgewise model of interface motion has been suggested to account for the observed phenomena.

Keywords: Orthoenstatite; Phase transformation; Raman spectroscopy; High pressure

1. Introduction

Pyroxenes are common mineral phases in many igneous and metamorphic rocks. Besides olivine, the iron (Fe^{2+})-bearing enstatite has been considered to be another major mineral phase in the Earth's upper mantle. Among the polymorphs of enstatite, only orthoenstatite (space group *Pbca*) and clinoenstatite (space group $P2_1/c$) occur naturally. Orthoenstatite is the high-temperature polymorph of clinoenstatite [1] and thus is metastable at ambient conditions. A pressure–temperature boundary between orthoenstatite and probably the high-pressure clinoenstatite (i.e., the so-called high-P $C2/c$ phase with space group $C2/c$) was determined experimentally 26 years ago [2]. However, the presence of the high-pressure clinoenstatite at upper mantle conditions was not verified by X-ray diffraction and crystal structure studies until the 1990s [3,4]. The orthoenstatite-to-high-pressure clinoenstatite transformation (i.e., the *Pbca*→high-P $C2/c$ transition) has been used to account for the cause of both Lehmann and the X-discontinuities observed in the upper mantle [4–6]. The stability of orthoenstatite at various temperatures and pressures is also important for its application in some low-voltage insulators, refractory and tough glass ceramics [7,8]. Therefore, the phase transition of orthoenstatite is of common interest to earth and materials scientists. This article reports Raman spectroscopic results of a pressure-induced metastable phase transformation in orthoenstatite at room temperature, focusing on the mechanism and order of the transition, as a comparison to the analog material, ferrosilite ($FeSiO_3$).

Enstatite, ferrosilite and their solid solutions have the same types of polymorphs. The phenomena observed in ferrosilite have been regarded to be the clues for predicting the behavior that may occur in enstatite. For the enstatite–ferrosilite system, the *Pbca*→high-P $C2/c$ transition was first observed in ferrosilite at 4.2 GPa and room temperature [9]. The analyses in microstructure and crystal structure of the recovered sample suggested that the *Pbca*→high-P $C2/c$ transition in ferrosilite is a first-order reconstructive transformation, and the high-P $C2/c$ phase retrogrades to low clinoferrosilite ($P2_1/c$) after relief of pressure [9].

*Fax: +886-2-2783-9871.
E-mail address: cclin@earth.sinica.edu.tw.

0022-4596/03/$ - see front matter © 2003 Elsevier Inc. All rights reserved.
doi:10.1016/S0022-4596(03)00278-0

The high-P $C2/c \rightarrow P2_1/c$ transition in enstatite was also testified by Raman spectroscopy of $MgSiO_3$ quenched from the stability field of high-P $C2/c$ phase [10]. Nevertheless, an *in-situ* X-ray diffraction study for the phase transition of orthoenstatite at room temperature has not been reported. Instead, the pressure-induced transition of orthoenstatite at room temperature has been estimated by Raman spectroscopy to occur at ~5 GPa [11] or ~9 GPa [12,13]. However, in contrast to what is observed in ferrosilite, Raman spectroscopic data show that the phase transition of enstatite is reversible at room temperature [11,13]. This raises the question: can the behavior found in the *Pbca*→high-P $C2/c$ transition of orthoferrosilite be directly applied to the case of orthoenstatite? To answer this question, Raman spectroscopic measurements at small pressure increment in the transition region were conducted back and forth to test the effectiveness for the analogy and to clarify the type and mechanism of the pressure-induced metastable phase transition.

2. Experimental

The orthoenstatite crystals used in this work were synthesized by means of the flux method developed by Ito [14]. The lithiumvanadomolybdate flux consists of Li_2O (51.2 mol%), MoO_3 (42.8 mol%), and V_2O_5 (6.0 mol%). SiO_2 and MgO in stoichiometric ratio were mixed with flux to obtain a 9 wt% of sample charge. The sample charge was put in a platinum crucible and heated up to 950±1°C, and then kept at this temperature for 170 h. The sample charge was then cooled slowly at a rate of 1.5°C/h to 650°C. Finally the furnace was switched off at 650°C, and the sample charge was allowed to cool in the furnace down to room temperature. The solvent was then washed off by soaking the charge in warm distilled water, and the insoluble products dried at ~100°C. The final products are $MgSiO_3$ crystals and $Li_2Si_2O_5$ (flaky and sometimes needle), as reported in literature [14,15]. The as-prepared $MgSiO_3$ crystals are colorless and transparent with a size of about 15–30 μm length and 5–15 μm width. A few bigger crystals with 100–500 μm in length were also found. The $MgSiO_3$ crystals were confirmed to be orthoenstatite by both powder (with step scan) and single-crystal X-ray diffraction. The cell parameters a, b, and c are 18.248 (4), 8.827 (2), and 5.185 (3) Å, respectively; where the values inside the parentheses are standard deviation. These data are slightly (<0.2%) larger than those reported in Ref. [14] and JCPDS card 19-768. The difference may be due to different amounts of impurities introduced by flux and/or systematic error of the diffractometer. Quantitative analysis by electron microprobe analysis (Jeol JXA-8900R at 15 kV and 45 s of collection time under wavelength-dispersive spectrum mode) showed that the major impurities as oxides in the as-prepared orthoenstatite are (in weight percentage) V_2O_3 (0.08±0.04) and MoO_3 (0.003±0.004). The potential impurity, lithium, cannot be reliably detected by the present microprobe analysis.

Except for minor differences in the frequency and number of bands below 700 cm^{-1}, the Raman spectra of clinoenstatite and orthoenstatite are very much alike. The bands with medium intensity at 344 and 371 cm^{-1} are the most discernible feature for clinoenstatite. These two bands have not been observed in orthoenstatite for several crystal orientations [16] nor in the orthoenstatite crystals of this study.

For the static compression experiments, one or two crystals of the sample, approximately 20–30 μm in size, were placed inside the hole (150 μm in diameter and 60–80 μm in depth) in a hardened stainless steel gasket that was put in a Mao–Bell-type diamond-anvil cell having anvil faces of approximate 600 μm in diameter. Each sample used in the pressure experiments was confirmed to be single crystal by using a polarizing microscope. Fine powders of ruby were also placed inside the hole, and deionized water was used as a pressure-transmitting medium. Below 1000 cm^{-1}, the Raman bands of ices VI and VII are weak and broad at various pressures and room temperature. Thus, the Raman bands of the pressure medium did not interfere with the recognition of sample signals. The whole assembly was then sealed by compressing the diamond anvils. It should be noted that the c-axis (the elongated crystal axis) of orthoenstatite crystal is always parallel to the culet of the anvil throughout the whole experiment. The orthoenstatite crystals were placed on top of the ruby powders, and the Raman spectra of samples and the ruby fluorescence spectrum were measured at the same spot. We have found this procedure tends to reduce the frequency errors caused by the pressure gradient across the crystals. Pressures were measured by using the ruby-fluorescence technique [17,18]. Several compression–decompression runs have been carried out. For each run, all spectra were collected from nearly the same position of a crystal. Note that hydrostaticity of the sample system was gradually lost with increasing pressure, especially at pressures higher than 10 GPa. However, based on the splitting of fluorescence bands of ruby, shear stress developed in the present sample was small throughout the pressure range studied. Thus, the experimental conditions were considered to be "quasi-hydrostatic" rather than "true hydrostatic".

The Raman spectra of samples at various pressures were carried out on a Renishaw-2000 Raman microprobe, and the back-scattering (180°) spectra were obtained with the 514.5 nm line from a Coherent Innova argon ion laser. All spectra were recorded with a Leitz UM 32 microscope objective and three accumulations at 300 s integration time with ~50 mW power on the

sample. The focused laser spot on the sample was estimated to be 2–4 μm in diameter. Wavenumbers are accurate to $\pm 1\,cm^{-1}$ as determined from plasma emission lines. The frequency of each Raman band reported in this study was obtained using Lorentzian curve fitting.

3. Results and discussion

3.1. Pressure dependence of Raman spectra

Some 45 Raman bands were recognized from different orthoenstatite crystals at ambient conditions. Thirty-three of them displayed observable pressure dependences and are listed in the first column of Table 1. However, one cannot observe all 45 Raman bands in a single measurement. The number of Raman-active modes in orthoenstatite is predicted to be 120 [19]. The reason for scarcity of the observed bands in a spectrum is attributed to weak intensity in many bands and overlap of some bands. For example, the ambient band at $927\,cm^{-1}$ significantly overlaps with the 935-cm^{-1} band (see also the 1-atm spectrum in Fig. 1a). It should be noted that the intensities of many Raman bands are orientation-dependent. For example, intensities of the ambient 664 and 1033-cm^{-1} bands are stronger than those of the 686 and 1011-cm^{-1} bands, respectively, at some orientations.

The pressure variations of the Raman frequencies of orthoenstatite were studied up to ~22 GPa at room temperature. Selected Raman spectra of orthoenstatite at various pressures and room temperature are shown in Fig. 1a. Fig. 1b shows the Raman spectra collected from decompression run. The Raman frequencies for all observable bands in both compression and decompression runs are plotted as a function of pressure in Fig. 2. To discriminate a mode from others, several symbols are used in the figure. The decompression data for adjacent bands are displayed alternately by plus (+) and cross (×). The solid lines (curves) in Fig. 2 are the regression lines (curves), while dashed lines are used for the highly uncertain data sets. Except for the ambient band at $852\,cm^{-1}$, which displays a concave upward frequency–pressure ($\nu-P$) plot, the frequencies of all observed Raman bands increase with increasing pressure.

Below 10 GPa, most of the Raman bands show nonlinear $\nu-P$ relationships. For the spectra obtained at pressures in excess of 10 GPa, a set of new bands accompanying with a discontinuity in the $\nu-P$ plots were observed. This phenomenon indicates that a phase transformation had taken place around 10 GPa. These new bands are marked by dots in Fig. 1a. Note that a half of the $\nu-P$ plots for the high-pressure phase appear to be nonlinear. Thus, both linear and quadratic regressions were used to fit the data sets, and the regression constants are listed in Table 1, the left five columns of the table for orthoenstatite, and the right four for the high-pressure phase. All regression data listed in Table 1 were based on the compression experiments. The details for phase transformation and the decompression data are discussed in the next section.

The nonlinearity in the $\nu-P$ plots (Fig. 2) below 10 GPa should not be caused by the development of shear stress in the sample because the system is nearly hydrostatic within this pressure range. Generally, non-hydrostaticity of a system in decompression experiment is more severe than that in compression experiment. However, during decompression, it is found that all Raman frequencies follow the $\nu-P$ trajectories obtained from compression run (the regression lines and curves in Fig. 2) and return to their ambient values. It should be noted that the 1-atm spectra (0.0001 GPa) shown in Figs. 1a and b have the same Raman bands. Therefore, a small to medium nonhydrostaticity developed in the samples does not considerably affect the vibrational frequencies of orthoenstatite within 10 GPa at least.

For compression of orthoenstatite and $(Mg,Fe)SiO_3$ orthopyroxenes at room temperature, it has been claimed that there is a change in compression mechanism at about 3 GPa [20], 4 GPa [12,21,22], or 5 GPa [13]. This behavior has been attributed to a change in compressibility of the SiO_4 tetrahedra—no change in Si–O distances and O–Si–O bond angles below 4 GPa, but regular shortening in Si–O distances and without angular distortion at higher pressures [12,22]. When the volume of a crystal is decreased by compression, the mode frequencies of a group of atoms (chemical bonds) may either increase or decrease, depending on the change of bond angles and bond lengths. Supposing that the SiO_4 tetrahedra in orthoenstatite are indeed incompressible below 4 GPa, the $\nu-P$ plots of Raman modes (especially the Si–O stretchings) should display a discontinuous change in slope at ~4 GPa. However, all Raman frequencies of orthoenstatite observed in this work show continuous and smooth shift with increasing pressure (Fig. 2) up to 10 GPa. The disappearance of several Raman bands below 6 GPa (Fig. 2) is attributed to very weak intensity at high pressures. Therefore, the present Raman data cannot confirm the argument that there is a change in compression mechanism of orthoenstatite at ~4 GPa. Raman spectroscopy may not be a good tool for identifying the compressional behavior of a type of polyhedron. However, on the basis of elasticity and sound velocities, Jackson et al. [23] and Flesch et al. [24] do not support the presence of a change in the pressure–volume trajectory of orthoenstatite at ~4 GPa either. Recently, on the basis of the pressure–volume data in Ref. [21], Angel (one of the co-authors in Refs. [12,21,22]) and Jackson [25] also used a line rather than two lines to describe the equation of state of orthoenstatite.

Table 1
Regression constants of enstatite for Raman bands determined in $\Delta v = v_0 + aP + bP^2$ at room temperature

	Orthoenstatite				High-pressure phase			
v_i[a]	v_0	a	$b \times 10^2$	R^2	v_0	a	$b \times 10^2$	R^2
83 s	83.4	2.36	−12.89	0.992	89.9	0.4		0.682
107 w	106.8	3.9	−30.0					
116 w	115.4	2.81		0.994	133.7	0.43		0.943
134 ms	134.3	4.77	−15.47	0.998	164.5	0.34		0.743
155 wm	155.3	0.5		0.794				
161 vw	161.5	0.4						
166 w	166.7	2.58	−10.03	0.994	161.7	1.31		0.978
197 wm	196.9	1.24	−5.73	0.966	187.1	0.83		0.923
206 wsh	206.5	2.31		0.988	201.5	2.29	−2.94	0.982
238 ms	238.2	1.96	−6.75	0.988	233.2	1.48		0.974
245 msh	244.8	3.60	−9.12		238.0	4.53	−13.24	0.839
					268.0	1.89		0.982
277 w	278.2	3.79	−14.86	0.986				
					307.9	0.84	−2.52	0.968
302 w	301.5	2.66		0.974	310.1	2.23		0.992
323 wsh	323.3	3.50	−11.93	0.982				
	327.7	4.36	−6.91	0.972	242.0	17.32	−48.07	0.992
					335.1	6.42	−12.94	0.978
343 svs	343.5	6.93	−16.22	0.998	321.5	9.76	−23.37	0.964
383 wm	383.8	2.75		0.962	377.3	4.31		0.972
					427.4	1.59		0.982
402 m	402.1	4.55	−8.25	0.992	407.7	2.73	−4.45	0.994
422 m	421.7	3.19	−8.86	0.992				
					377.1	10.70	−28.50	0.980
446 w	445.5	2.44	−1.04	0.992	443.1	2.67		0.992
459 vw	458.8	3.33	−11.80	0.992	407.7	9.64	−20.12	0.982
474 vw	472.9	2.66		0.994				
524 m	524.9	2.50		0.990	513.0	4.53	−6.31	0.951
					566.4	0.98		0.740
552 m	551.5	2.62		0.990				
580 m	580.3	1.80		0.945				
595 vw	594.5	6.23	−36.26	0.992				
					660.1	3.52		0.960
664 svs	663.8	3.87	−5.03	0.998	668.9	3.92	−1.10	0.992
686 vs	686.1	3.83	−6.90	0.998	684.1	4.31	−1.17	0.994
750 w	750.7	2.32	−10.14	0.986				
					816.9	2.8		
852 m	851.1	−0.12	18.89	0.984	806.4	8.27	−13.36	0.978
					912.6	0.97		0.780
927 m	926.6	3.84	−6.31	0.996	927.3	2.43	−1.54	0.968
935 w	935.2	6.25	−12.61	0.998				
					979.1	7.37	−10.08	0.992
1011 vs	1011.3	6.79	−16.14	0.996	986.2	8.76	−14.31	0.988
1033 svs	1032.9	6.28	−13.39	0.998	1037.0	4.66	−1.25	0.982

v_i, v_0 and Δv are in cm^{-1}, P in GPa, and the constants, a and b have the corresponding units. v_i is the frequency measured at ambient conditions. R^2 is the correlation coefficient.

[a] vs = very strong, svs = strong–very strong, s = strong, ms = medium–strong, m = medium, wm = weak–medium, w = weak, vw = very weak, sh = shoulder.

3.2. Phase transformation

As shown in Figs. 1a and 2, a new set of spectra appears when pressure is increased to about 10 GPa. The Raman bands of orthoenstatite disappear completely at ~11 GPa. All Raman frequencies of the high-pressure phase increase monotonically with increasing pressure (Fig. 2), and a further another $v-P$ discontinuity was not observed up to 22 GPa. Both Raman spectra and the outline of $v-P$ plots of the high-pressure phase are basically identical to those reported in literature [13]. For example, 29 of the 31 Raman bands of the high-pressure phase (see Table 1 and Fig. 2) show nearly the same frequencies as those reported in Ref. [13] at 12.5 GPa. The remaining two extra bands can be attributed to difference in crystal orientation for the two

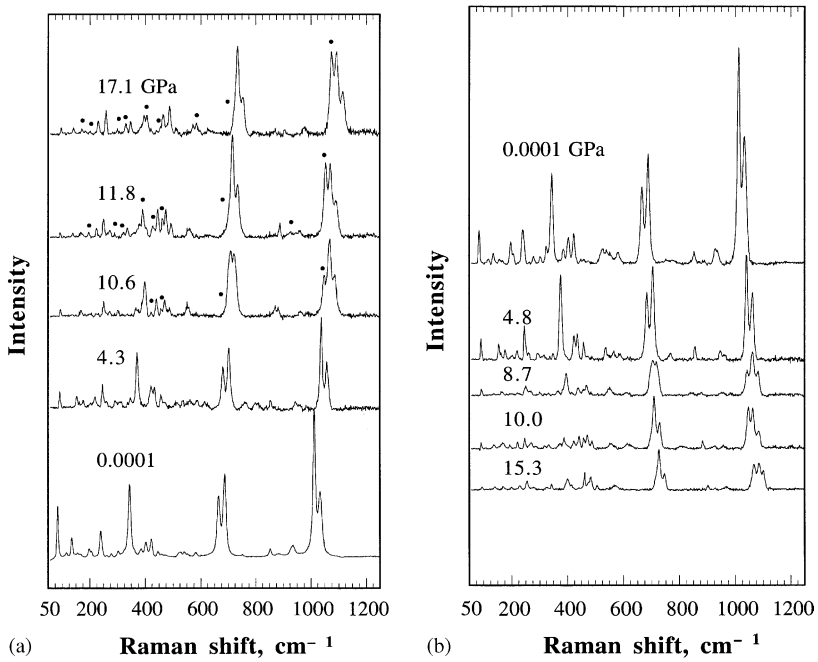

Fig. 1. Raman spectra of orthoenstatite as a function of pressure at room temperature: (a) spectra collected during compression, and (b) spectra obtained from decompression run. In (a), the new bands from the high-pressure phase are marked by dots. The full scale in (a) is 3/4 of that in (b).

studies. By comparing with the spectrum of diopside and $MgGeO_3$ (two clinopyroxenes with space group of $C2/c$) at the same pressure, Chopelas and Boehler [11] and Chopelas [13] claimed that the high-pressure phase is of $C2/c$ symmetry.

The regression constants for the fitted $v-P$ plots of the high-pressure phase are listed in the right four columns of Table 1. These constants are generally not identical to those reported by Chopelas [13]. This inconsistency is chiefly because: (a) a half of the $v-P$ trajectories of the high-pressure phase in this work appears to be nonlinear, but only linear regression was adopted in Ref. [13], (b) different pressure ranges were taken for data fitting, 11–22 GPa in this work but ~6–25 GPa in Ref. [13], (c) the data in Table 1 were obtained from compression experiments, but both compression and decompression data may be used for fitting in Chopelas's work. (Note that the method for data fitting was not mentioned in [13].)

When pressure is released, the high-pressure phase remains stable down to ~9.5 GPa, and then gradually transforms back to orthoenstatite. The high-pressure phase cannot be retained at ambient conditions. Therefore, this is a reversible phase transition and is consistent with that observed in Ref. [13]. It should be noted that some Raman frequencies form hysteresis loops in the $v-P$ plane during transition, e.g., the ambient bands at 197, 206, 238, 664, 686, 852, 1011, and 1033 cm^{-1} (Fig. 2). The ambient bands at 1011 and 1033 cm^{-1} are the most intense and reliable signals in this regard. The beginning of phase change can be easily recognized by the appearance of a new band beside the ambient 1011-cm^{-1} band (i.e., the highest frequency band among the dot-marked bands in Fig. 1a). It has been visually observed that the crystals did not rotate during phase transition, and that the intensity ratios of the two strong Raman bands ($I_{(1011)}/I_{(1033)}$) showed small variation throughout the whole experiment (Fig. 3). Suppose that the variations of relative polarizabilities between the ambient 1011 and 1033-cm^{-1} bands can be neglected in the pressure range studied, and that the modes of the two bands do not change after phase transition; then, one can estimate the amount or degree of transition at various pressures based on peak areas of the concerned Raman bands. On the basis of this assumption, Fig. 4 displays the pressure dependence of transition percentage in orthoenstatite crystals. Obviously, the forward and reverse transitions also form a hysteresis loop in the transition percentage–pressure plane. It should be noted that an abnormal $I_{(1011)}/I_{(10323)}$ ratio across the transition region (8–11 GPa) in the compression run (Fig. 3) has been observed. This phenomenon may involve unequal changes in polarizability of the ambient 1011 and 1033-cm^{-1} bands as a result of interaction with the new vibrational mode in a specific crystal orientation and pressure. Alternatively, this may have something to do with activation volume difference of an intermediate phase for the compression vs. decompression route, as shown experimentally for solid–solid transformations in nanocrystals [26].

It is also noteworthy that there are no appreciable changes in color, shape and microstructures for $MgSiO_3$

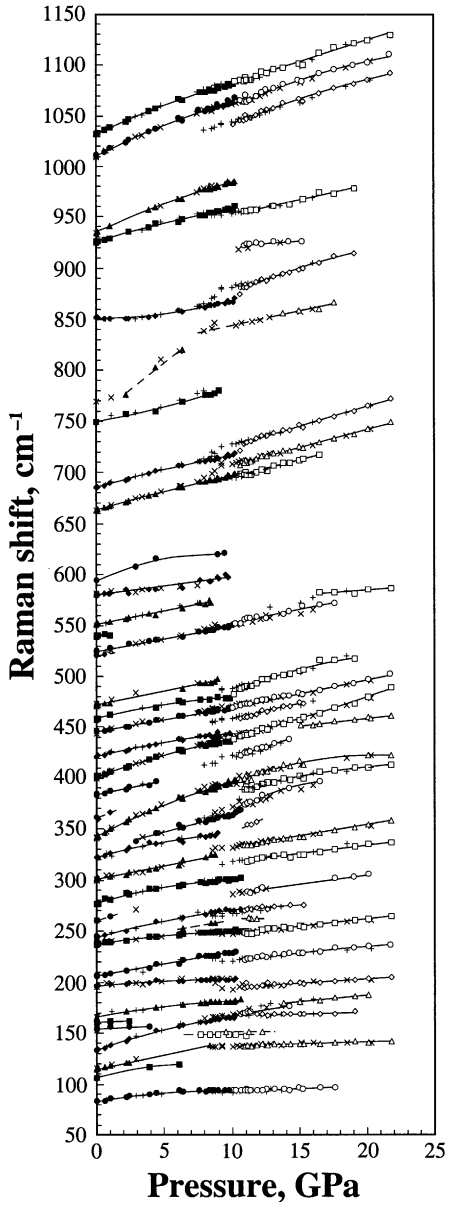

Fig. 2. Pressure dependence of Raman frequencies at room temperature. Solid and open symbols denote the data of orthoenstatite and the high-pressure phase, respectively for compression runs. Plus (+) and cross (×) represent the data collected from decompression runs.

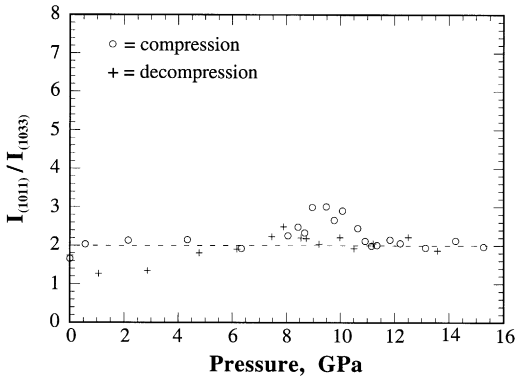

Fig. 3. The intensity ratios $I_{(1011)}/I_{(1033)}$ of the Raman bands as a function of pressure. The intensities $I_{(1011)}$ and $I_{(1033)}$ represent the peak areas of the bands derived from the ambient 1011 and 1033-cm^{-1} bands, respectively. Note that the crystals did not rotate in the pressure range of 4–16 GPa.

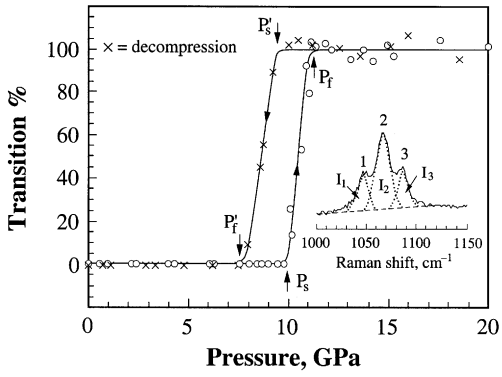

Fig. 4. Pressure dependence of transition percentage for the high-pressure polymorph of orthoenstatite at room temperature. The inserted spectrum illustrates the bands for calculation: band 1 is the new band, and bands 2 and 3 are derived from the ambient 1011 and 1033-cm^{-1} bands, respectively. Intensities I_1, I_2, and I_3 are the corresponding peak areas of the three bands. The transition percentage is defined to be $100I_1/0.41(I_1+I_2+I_3)$, where 0.41 is the average $I_1/(I_1+I_2+I_3)$ ratio based on the data obtained from P 12 GPa. P_s and P'_s denote the initial pressures for the forward and reverse transitions, respectively, and P_f and P_f' the end pressures for phase transition.

crystals during transitions. The crystals remained intact without cracking throughout the forward and reverse transitions. The crystal recovered from high pressure (>10 GPa) remained as a single crystal at ambient conditions. Recently, a phase boundary sweeping a crystal from one side to another during compression was reported for the displacive $P2_1/c \rightarrow$high-P $C2/c$ transition of spodumene [27]. This phenomenon was not observed in this study. Nevertheless, the transition was characterized by the relative intensity of the new band and the two old bands (i.e., bands 2 and 3 in the inset of Fig. 4) changing at once at each pressure increment, and then remained unchanged at that pressure for several days. That is to say, the transition percentage (i.e., $100I_1/0.41(I_1+I_2+I_3)$ in Fig. 4) at a given pressure and room temperature is time-independent. In this study, all spectra were collected from nearly the same position of the crystal for each run. It should be impossible that a crystal position has different extent of transformation at various pressures. Therefore, the transition percentages in Fig. 4 may reflect the extent of deformation in the unit cell of orthoenstatite. The time-independent transition percentage implies that the deformation is elastic if creep of crystal at room temperature can be ignored. Thus, the phase transition observed in the present orthoenstatite crystal is probably displacive or second order in nature and most likely involves an elastic distortion of crystal structure. On the

other hand, the $Pbca \rightarrow$ high-P $C2/c$ transition in ferrosilite was reported to be a first-order reconstructive transformation [9]. The discrepancy leads to the question as to whether the high-pressure phase of orthoenstatite is indeed the high-P $C2/c$ phase as that claimed by Chopelas and Boehler [11] and Chopelas [13] and casts doubt on the type of phase transition as further addressed in the next section.

3.3. A consideration on the transition type and mechanism—first order or second order?

The major features for the present transition at room temperature are: (a) the transition percentage of the resultant phase (i.e., the high-pressure phase for compression run and orthoenstatite for decompression run) is time-independent for a few days at a given pressure and (b) the amount of resultant phase shows a sigmoid relationship with pressure. A hysteresis loop (or two sigmoid curves) in the transition amount is common in thermally induced phase transformation of many polycrystalline solids, e.g., martensitic transformation in ZrO_2 [28] and steel [29]. This phenomenon has been regarded as an indicator for a first-order solid-state phase transition, and has been attributed to nonsimultaneous nucleation in different particles of the sample [30], the existence of a kinetic barrier for nucleation or the strain energy stored in the hybrid crystals [31]. The hysteresis of thermally activated transition in these polycrystalline materials cannot be simply applied to the case of orthoenstatite at high pressure because the transition % data (Fig. 4) in the present enstatite were collected from specified position of the crystal. According to Landau theory [31], a continuous change in transition percentage for the same position of a crystal should be accompanied by a second-order transition. The pressure-induced phase transition in orthoenstatite with hysteresis loop for a specified position on the single-crystal sample seems to be both first-order and second-order. However, such a hybrid "first–second" order phase transition is not permitted from the viewpoint of thermodynamics.

For a second-order (or displacive) phase transition, it needs a cooperative and homogeneous process involving simultaneously all constituent particles in the bulk. This implies that a continuous change in symmetry of crystal structure has to take place during a second-order phase transition. Recently, an X-ray study using a synchrotron source has not revealed an intermediate structure between orthoenstatite and its high-pressure polymorph. Actually, the X-ray diffraction pattern at 10.4 GPa (ca. the middle point of the sigmoid curve) is only of the high-pressure polymorph [32]. For a second-order (or displacive) solid-state phase transition, it is also impossible that a sudden formation of the resultant phase followed a gradually isotropic distortion in crystal structure of the initial phase. Therefore, the pressure-induced phase transformation in orthoenstatite should be first-order or reconstructive. This conclusion is consistent with that claimed for the $Pbca \rightarrow$ high-P $C2/c$ transition in ferrosilite [9]. However, the phase transition in orthoenstatite is reversible, which is at variance with that observed in the pressure experiment for orthoferrosilite and the quenching experiment for the high-P $C2/c$ phase [9,10]. Recently, the room-temperature Raman spectra of the high-pressure polymorphs of both orthoenstatite and clinoenstatite reported in Refs. [11,13,33], and the present work were compared to one another at 12.5 GPa. It is found that the number of Raman bands and frequency for the high-pressure polymorphs of orthoenstatite observed in Ref. [13] are highly consistent with those observed in this study. A high similarity between the Raman spectra of the high-pressure polymorphs of clinoenstatite reported in Refs. [11,33] is also found. However, a significant difference between the Raman spectra of the two high-pressure polymorphs has suggested that the high-pressure polymorph of orthoenstatite is not the so-called high-P $C2/c$ phase [33]. From the pressure–temperature ($P-T$) phase diagram of ferrosilite, both clinoferrosilite and orthoferrosilite have the same high-pressure polymorph with $C2/c$ structure [6]. It is likely that the high-pressure polymorph observed in this study may have a transition structure between those of orthoenstatite and the high-P $C2/c$ phase if the relationship found in ferrosilite can be applied to enstatite. In such a case, the high-pressure polymorph of orthoenstatite is a metastable phase at room temperature and high pressure and may not have a stable $P-T$ field. On the other hand, Yang and Prewitt [34] have considered that orthoenstatite may transform to a phase with structure $P2_1ca$ at pressures above 8.5 GPa. Therefore, it is possible that the present high-pressure phase is the so-called $P2_1ca$ phase and has its stability field in the $P-T$ plane.

The molar volume of the high-pressure polymorph of orthoenstatite has not been reported. The volume change for transition of enstatite from $P2_1/c$ (clinoenstatite) to the $C2/c$ symmetry at room temperature and 5–6 GPa was reported to be 2.7–3.1% [5,21]. On the other hand, the volume change for the $Pbca \rightarrow$ high-pressure $C2/c$ transition in ferrosilite at room temperature is $\sim$2.6% [9]. It is known that the difference between the molar volume of clinoenstatite and orthoenstatite is less than 0.5% at ambient conditions. Therefore, the volume change in the pressure-induced phase transition of orthoenstatite may be as small as 2% or less if the high-pressure polymorph of orthoenstatite is the intermediate phase between orthoenstatite and the high-P $C2/c$ enstatite. The fact that the formation of crack was not observed in crystals during both the forward and reverse transitions supports the above inference.

It is known that the intensity of a Raman band is a function of crystal orientation. Therefore, the prerequisite for obtaining a reliable transition percentage based on Raman intensity is that the crystal orientation and the modes of the relevant Raman bands remain constant during transition, as indeed is the case in this study. Suppose the collection depth for Raman spectroscopy in the present sample is always deep enough (about 20 μm) to cover the interphase interface for a first-order transition; then, the edgewise model of interface motion suggested by Mnyukh [30] can be extended to the present transition as follows: (a) the applied pressure may induce a number of nuclei, e.g., dislocations or the vacancy agglomerates suggested by Mnyukh, in the initial phase (i.e., orthoenstatite for compression run and the high-pressure polymorph for decompression run), (b) these nuclei are then removed by movement of the interface via a process similar to the ledge-shifting mechanism in crystal growth and dissolution during growth of the resultant phase. The annihilation of nuclei by movement of the interface will result in a time-independent amount of the resultant phase at a given pressure. At that time, the interface also ceases to move. The movement of the interface must be so fast as to obtain the apparent "instant growth" of the resultant phase. A further increase (or decrease) in pressure should cause the formation of other nuclei, movement of the interface and finally an increase in transition percentage. In this transition mechanism, the migration of the interphase interface rather than layered antiphase boundaries or alternate layers of the resultant and initial phases is of relevance to time-independent transition percentages at the specified position in a crystal. The interphase interface moving along the observation direction is essential for this hypothetical mechanism. However, an interphase interface perpendicular to the observation direction cannot be optically observed in the present experiment. In any case, to trigger a pressure-induced phase transition, a driving force for nucleation analogous to undercooling or superheating in a thermally induced phase transition is necessary. In this connection, the metastable equilibrium pressure for transition can be estimated to be between 9.5 and 10 GPa by using the two sigmoid transition %–pressure curves.

3.4. Effects of impurity cations and shear stress

In Fig. 4, the phase transition of orthoenstatite apparently starts at 10 GPa (P_s) and terminates at ~11 GPa (P_f) for compression runs, while it starts at ~9.5 (P_s') and finishes at ~7.5 GPa (P_f') for the reverse transition. It has been predicted that the pressure for triggering the $Pbca \rightarrow$ high-P $C2/c$ transition of enstatite can be lowered by the addition of Fe^{2+} [6]. This motivates us to study the effect of transition metal cations on the phase transition of orthoenstatite. Several M^{2+}-doped orthoenstatites (M = Mn, Fe, Co, Ni) have been synthesized by the same method described in Section 2. The effect of M^{2+} cations on the transition pressure (P_s) turns out to be rather minor, within 10 wt% of addition, for the forward transition. For example, P_s was lowered by only ~0.2 GPa in the doped orthoenstatite with 7 wt% of NiO and 9 wt% of FeO. On the other hand, the end pressure (P_f') for the reverse transition was significantly lowered (e.g., down to 5.5 GPa) when a large pressure gradient was developed in the crystal during decompression. This fact indicates that the high-pressure phase can be stabilized at lower pressure by shear stress. As a result of such a nonhydrostaticity, the shape of the transition percentage–pressure loop was significantly modified for back-transformation. However, nonhydrostaticity does not cause a significant shift in Raman frequencies, as already mentioned.

The significant effect of shear stress on P_f' may not necessarily imply a displacive phase transition. Shear stress developed in the sample may inhibit the nucleation of orthoenstatite from the high-pressure phase. A lower transition pressure for orthoenstatite at room temperature reported in literature [11–13] may be partly attributed to the development of shear stress if the high-pressure phase in these systems is identical to that in this study.

4. Conclusions

The compressional behavior of a synthetic orthoenstatite under quasi-hydrostatic conditions have been studied up to ~22 GPa at room temperature. Except the ambient 852-cm^{-1} band of orthoenstatite, all the frequencies of Raman bands increase with increasing pressure. Below 10 GPa, neither the lattice modes nor the internal modes of SiO_4 have a discontinuous change in slope of the $\nu - P$ plots. The continuous and smooth frequency shift in Raman modes does not confirm the argument that the SiO_4 tetrahedra are incompressible within 4 GPa.

At 10 GPa, orthoenstatite begins to transform to a high-pressure phase. The forward phase transition finishes at 11–12 GPa. Above 10 GPa, all the frequencies of Raman bands increase with increasing pressure again, and a further transition was not found up to ~22 GPa. Upon decompression, the high-pressure phase remained stable down to ca. 9.5 GPa, and then gradually transformed back to orthoenstatite. Only orthoenstatite was observed at pressures below 7 GPa. This result indicates that the high-pressure phase cannot be preserved at ambient conditions. The phase transformation in an orthoenstatite single crystal at room temperature has the following features:

(a) The transition is reversible but has a hysteresis in both Raman frequency–pressure and transition percentage–pressure planes.

(b) The transition percentage collected for a specified position of the crystal is time-independent at a given pressure.
(c) There was no appreciable cracking or change in color and shape of the enstatite crystals for both the forward and reverse transitions. The sample recovered from high pressure rejuvenates as a single-crystal orthoenstatite.

The transition type has been inferred to be of first order. However, the pressure-induced polymorph for orthoenstatite at room temperature is not the same as the high-P $C2/c$ phase for the analog ferrosilite. Instead, the high-pressure polymorph observed in this study may be an intermediate between orthoenstatite and the high-P $C2/c$ phase. The observed transformation behavior can be interpreted in terms of a mechanism based on Mnyukh's edgewise model of interface motion. In comparison with the effect of an applied shear stress, doping metal cations, e.g., Fe^{2+} and Ni^{2+}, showed rather minor influence on the transition pressure within 10 wt% of addition.

Acknowledgments

This work is supported by NSC Grant 89-2116-M-001-020, Taiwan, ROC. The author thanks Prof. P. Shen for helpful discussion of the manuscript. The assistance of Mr. H.D. Chiang, Institute of Materials Science and Engineering of National Sun Yat-Sen University and Ms. S.F. Dong, Department of Earth Sciences of National Cheng Kung University in analyses of the composition of samples and single-crystal X-ray diffraction, respectively, is gratefully acknowledged.

References

[1] W.A. Deer, R.A. Howie, J. Zussman, An Introduction to the Rock-Forming Minerals, 2nd Edition, Longman Sci. & Tech, Essex, 1992.
[2] K. Yamamoto, S. Akimoto, Am. J. Sci. 277 (1977) 288–312.
[3] R.E.G. Pacalo, T. Gasparik, J. Geophys. Res. B 95 (1990) 15853–15858.
[4] R.J. Angel, A. Chopelas, N.L. Ross, Nature 358 (1992) 322–324.
[5] M.J. Mendelssohn, G.D. Price, Phys. Chem. Minerals 25 (1997) 55–62.
[6] A.B. Woodland, R.J. Angel, Eur. J. Mineral. 9 (1997) 245–254.
[7] L.M. Echeverria, G.H. Beall, Ceram. Trans. 20 (1991) 235–244.
[8] E. Medvedovski, Interceramics 45 (1996) 85–86.
[9] D. Hugh-Jones, T. Sharp, R. Angel, A. Woodland, Eur. J. Mineral. 8 (1996) 1337–1345.
[10] P. Ulmer, R. Stalder, Am. Mineral. 86 (2001) 1267–1274.
[11] A. Chopelas, R. Boehler, in: Y. Syono, M.H. Manghnani (Eds.), High-Pressure Research: Application to Earth and Planetary Sciences, Terra Scientific, Tokyo, 1992, pp. 101–108.
[12] D. Hugh-Jones, A. Chopelas, R. Angel, Phys. Chem. Minerals 24 (1997) 301–310.
[13] A. Chopelas, Am. Mineral. 84 (1999) 233–244.
[14] J. Ito, Geophys. Res. Lett. 2 (1975) 533–536.
[15] F.C. Hawthorne, J. Ito, Can. Mineral. 15 (1977) 321–338.
[16] H. Mao, R.J. Hemley, E.C.T. Chao, Scanning Microsc. 1 (1987) 495–501.
[17] H.K. Mao, P.M. Bell, J.W. Shaner, D.J. Steinberg, J. Appl. Phys. 49 (1978) 3276–3283.
[18] H.K. Mao, J. Xu, P.M. Bell, J. Geophys. Res. B 91 (1986) 4673–4676.
[19] J.R. Ferraro, Appl. Spectrosc. 29 (1975) 418–421.
[20] A. Chopelas, EOS Trans. Am. Geophys. Union 69 (1988) 472.
[21] R.J. Angel, D.A. Hugh-Jones, J. Geophys. Res. B 99 (1994) 19777–19783.
[22] D.A. Hugh-Jones, R.J. Angel, Am. Mineral. 79 (1994) 405–410.
[23] J.M. Jackson, S.V. Sinogeikin, J.D. Bass, Am. Mineral. 84 (1999) 677–680.
[24] L.M. Flesch, B. Li, R.C. Liebermann, Am. Mineral. 83 (1998) 444–450.
[25] R.J. Angel, J.M. Jackson, Am. Mineral. 87 (2002) 558–561.
[26] K. Jacobs, D. Zaziski, E.C. Scher, A.B. Herhold, A.P. Alivisatos, Science 293 (2001) 1803–1806.
[27] T. Arlt, R.J. Angel, Mineral. Mag. 64 (2000) 241–245.
[28] E.C. Subbarao, in: A.H. Heuer, L.W. Hobbs (Eds.), Science and Technology of Zirconia, Amer. Ceram. Soc. Inc, Columbus, OH, 1981, pp. 1–25.
[29] J.W. Christian, The Theory of Transformations in Metals and Alloys—Equilibrium and General Kinetic Theory, Pergamon Press, Oxford, 1975.
[30] Y. Mnyukh, Fundamentals of Solid-State Phase Transitions, Ferromagnetism and Ferroelectricity, 1st Books Library, IN, 2001.
[31] C.N.R. Rao, K.J. Rao, Phase Transitions in Solids—An Approach to the Study of the Chemistry and Physics of Solids, McGraw-Hill, New York, 1978.
[32] C.M. Lin, J.L. Chao, C.C. Lin, Metastable phase transition of orthoenstatite ($MgSiO_3$) under high pressure, Appl. Phys. A, 2003, submitted for publication.
[33] C.C. Lin, Pressure-induced polymorphism in enstatite ($MgSiO_3$) at room temperature: clinoenstatite and orthoenstatite, J. Chem. Phys. Solids, 2003, submitted for publication.
[34] H. Yang, C.T. Prewitt, in: R.M. Hazen, R.T. Downs (Eds.), High-Temperature and High-Pressure Crystal Chemistry, The Mineralogical Society of America, Washington, DC, 2000, pp. 211–255.